Supplementary Information

Microfluidic device for mechanical dissociation of cancer cell aggregates into single cells

Xiaolong Qiu[1,†], Janice De Jesus[1,†], Marissa Pennell[1], Marco Troiani[1], and Jered B. Haun[1,2,3,*]

[1] Department of Biomedical Engineering, University of California Irvine, Irvine, CA 92697

[2] Department of Chemical Engineering and Materials Science, University of California Irvine, Irvine, CA 92697

[3] Chao Family Comprehensive Cancer Center, University of California Irvine, Irvine, CA 92697

[†] These authors contributed equally to this work

*Jered B. Haun, PhD

Department of Biomedical Engineering

University of California Irvine

3107 Natural Sciences II

Irvine, CA, 92697

949-824-1243

jered.haun@uci.edu

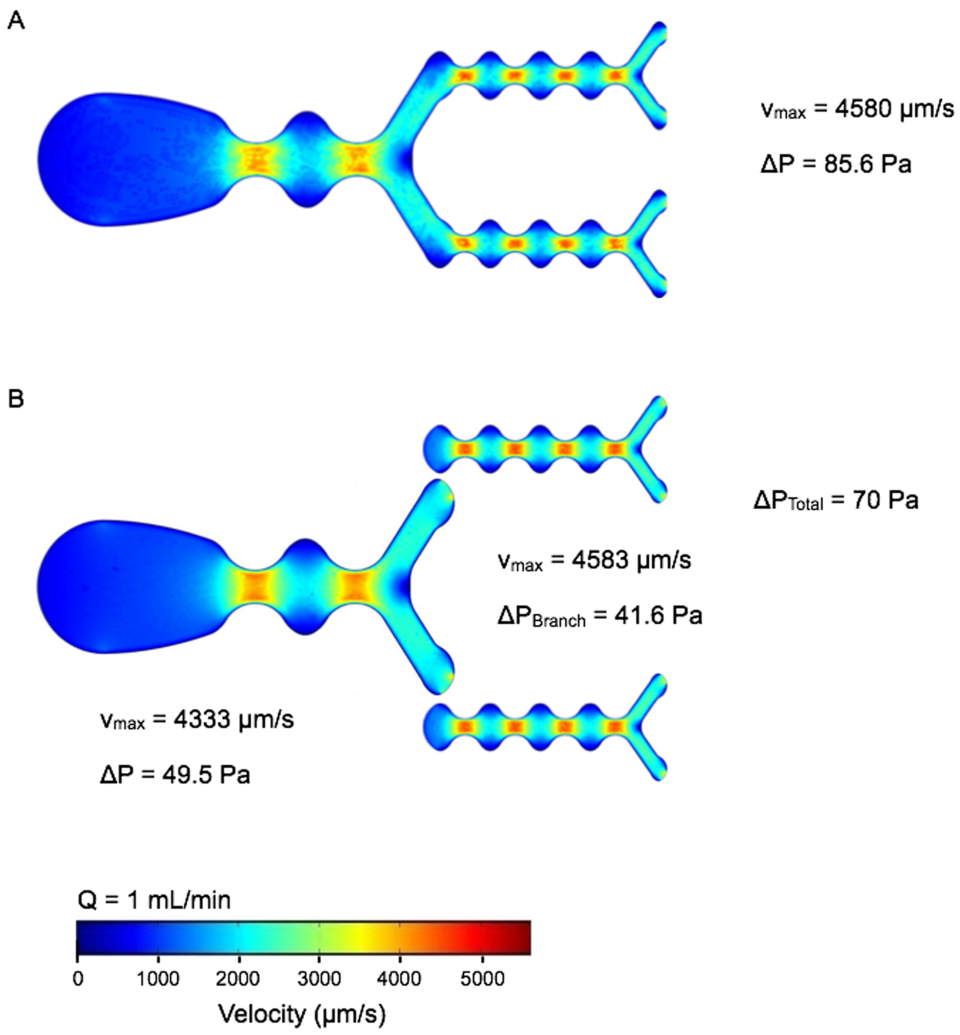

Figure S1. Finite-element fluid dynamics simulations of single and consecutive stages. Simulations were performed at 1 mL/min flow rate for the first and second device stages (A) with direct connection between the stages or (B) as separate units. Inlet conditions for stage 2 in part B are based on the average velocity. Velocity profiles appear similar, and the maximum velocity values are identical. Separating the stages does however lead to underestimating the total pressure drop by 15%.

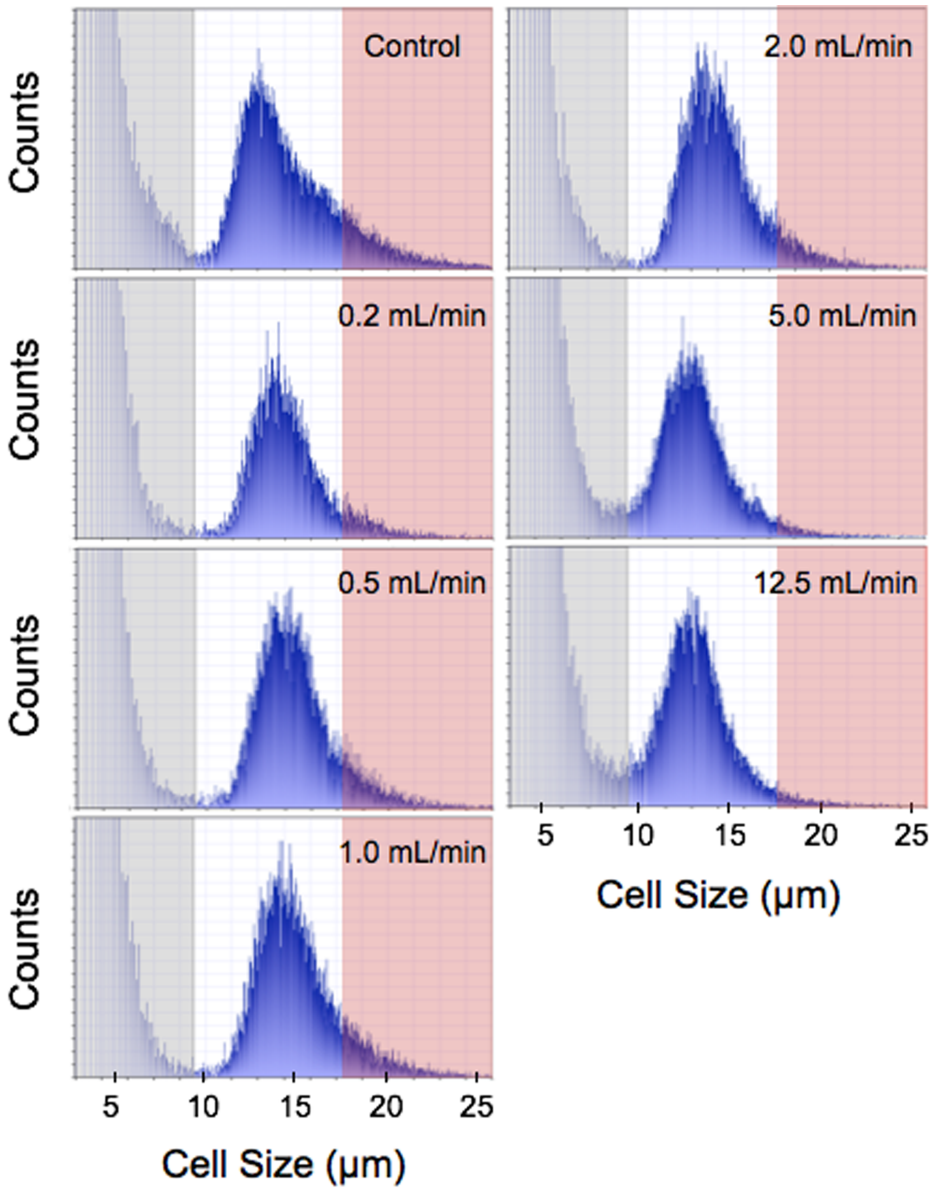

Figure S2. HCT 116 cell suspensions passed through the dissociation device at different flow rates. Representative cell counter histograms obtained before (control) and after passing through the microfluidic device under the indicated flow rate conditions. The population gradually became evenly distribute around the average cell size of 13.5 µm diameter, as larger clusters were dissociated.

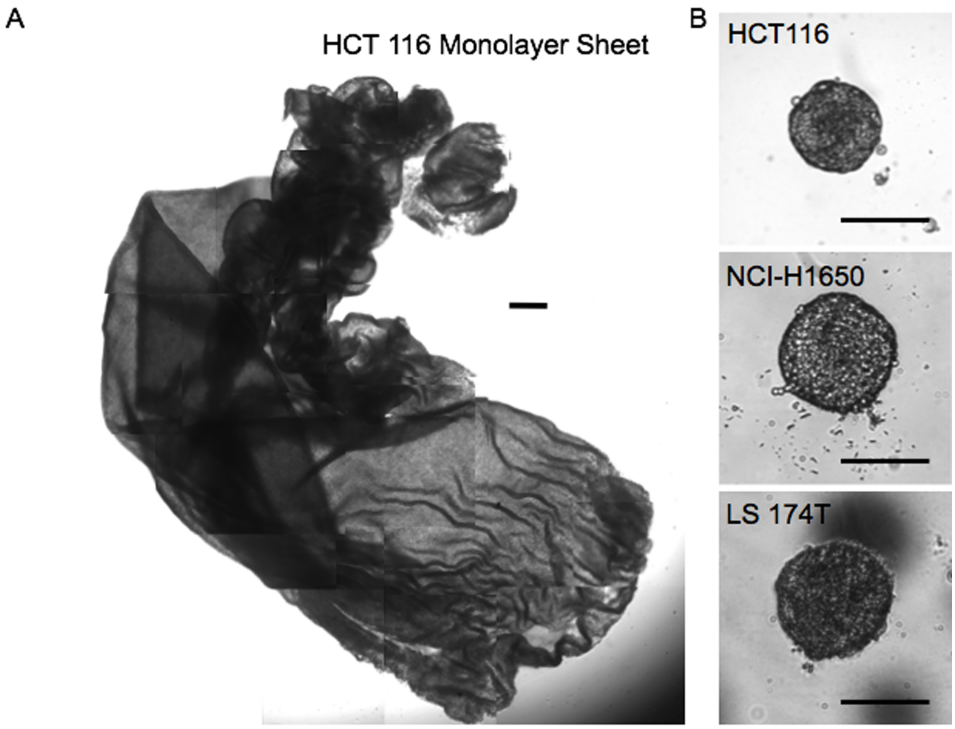

Figure S3. Tumor monolayer sheet and spheroid models. (A) Tumor monolayer sheet created by growing HCT 116 cells in collagen coated 24 well plates and releasing with collagenase. Image was manually tiled together from many individual micrographs. (B) Tumor spheroids produced using the hanging drop method for HCT 116, NCI-H1650, and LS 174T cells. Scale bars represent 250 μm.

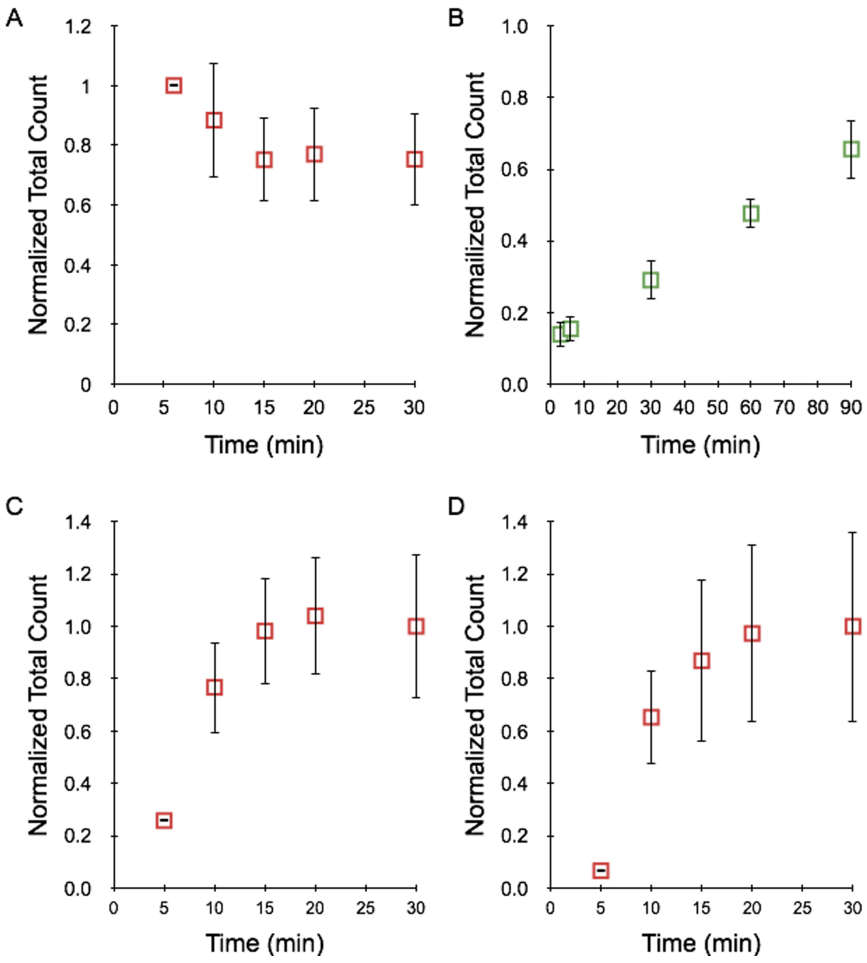

Figure S4. Tumor spheroid dissociation time-courses for trypsin and EDTA treatments. Tumor spheroids were treated with trypsin-EDTA or EDTA and cell counts were taken at different time points. (A) HCT 116 spheroid digestion with trypsin was maximal at 5 min and actually decreased after this point, most likely due to cell sensitivity. (B) EDTA treatment was much less efficient, reaching 50% of the maximum level from trypsin digestion after an hour, and continuing to increase with further incubation. (C) NCI-H1650 and (D) LS 174T spheroids were more difficult to digest with trypsin, requiring 20 min to reach maximal dissociation. All results were normalized to the maximum count determined from trypsin digestion for each spheroid type. Error represent the standard error from at least three independent experiments.

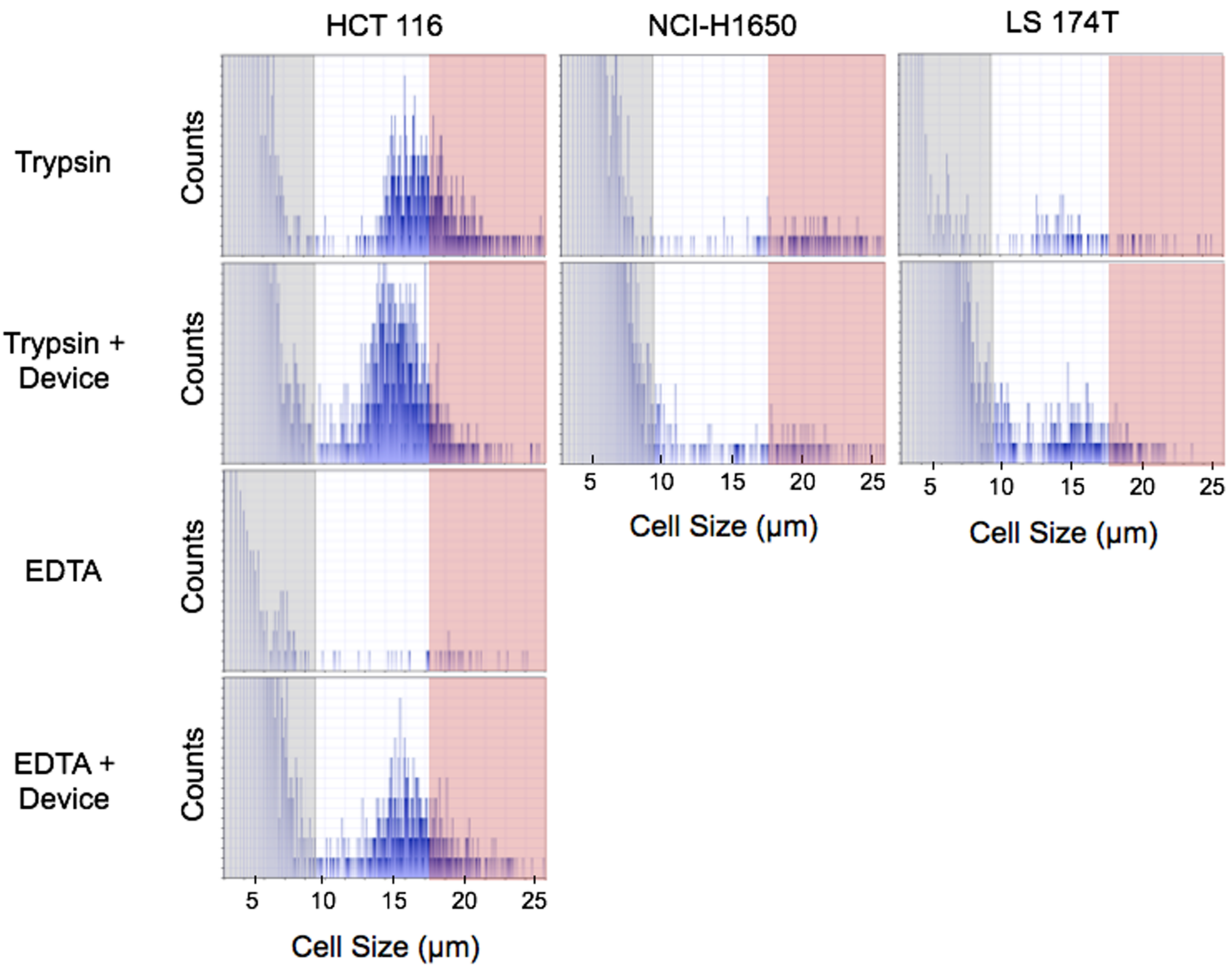

Figure S5. Cell counter histograms for dissociated tumor spheroids. Representative cell distributions measured for different tumor spheroid types following treatment with trypsin, EDTA, or these treatments in combination with microfluidic dissociation at 12.5 mL/min for 10 passes. Note that mean cell diameters were larger for spheroid samples (16 μm for HCT 116 and LS174T, 17 μm for NCI-H1650), so single cell gates were shifted accordingly.

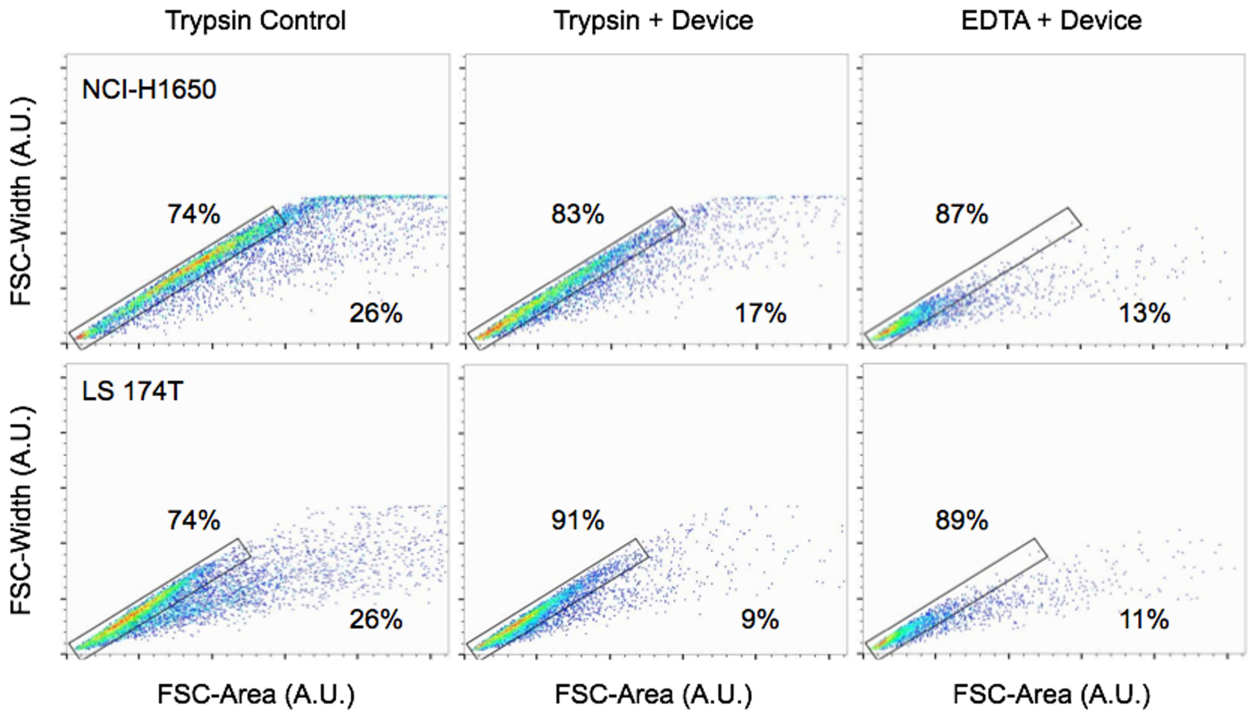

Figure S6. Flow cytometry analysis of single cells and aggregates obtained from tumor spheroids. Single cells are identified following dissociation of NCI-H1650 and LS 174T spheroids by plotting forward scatter (FSC)-width versus FSC-area. Single cells are shown in the boxed region, with the larger and non-symetric aggregates outside.

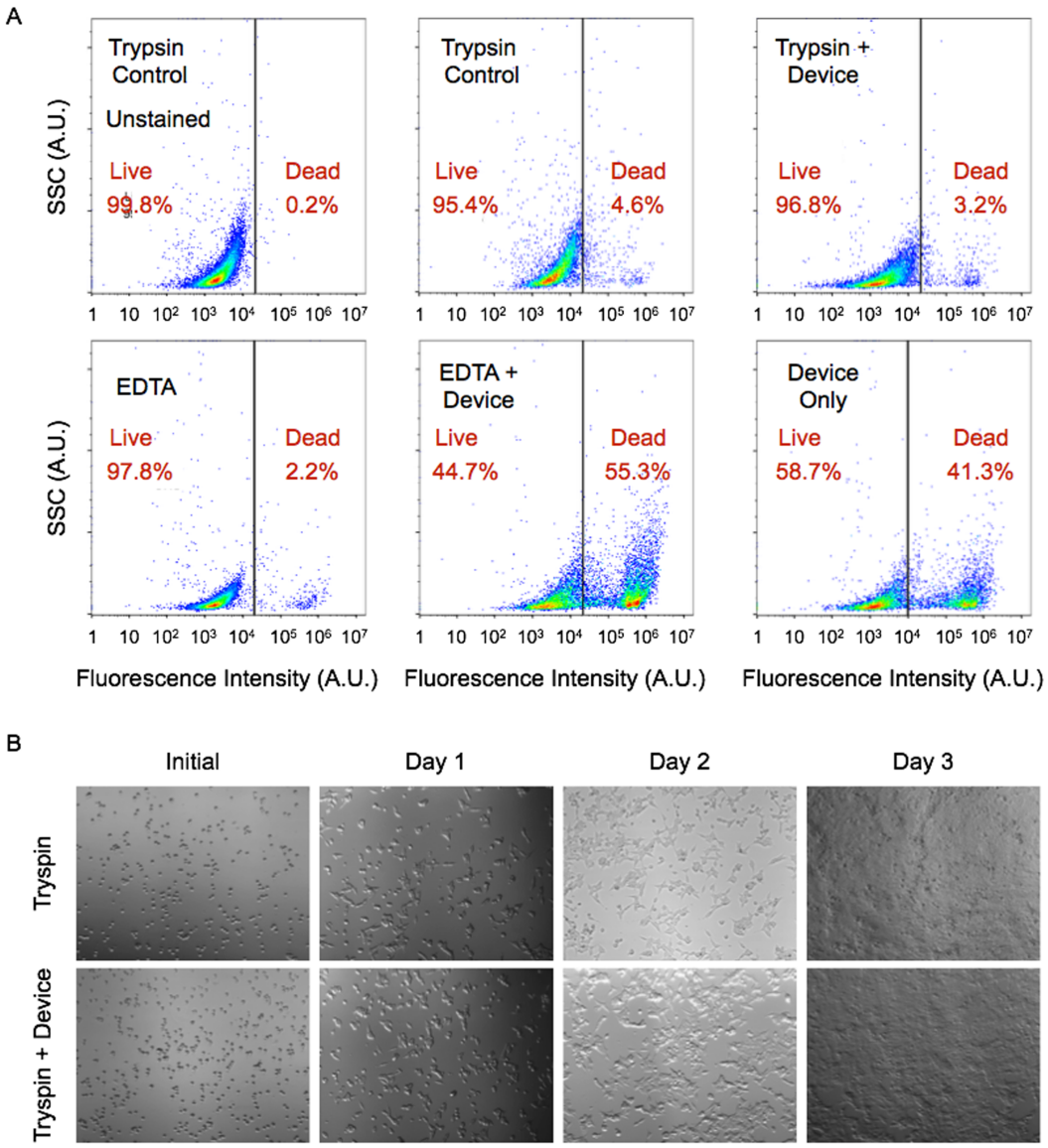

Figure S7. Cell viability studies. (A) Representative flow cytometry histograms for showing PI fluorescence for HCT 116 cells following the indicated dissociation conditions. Live cells were gated based on the trypsin-treated control, with a cut off just beyond a signal of 10,000. The percentage of live cells that were averaged over separate experiments are shown in Figure 6B. (B) Micrographs showing growth of HCT 116 cells after treatment of spheroids using trypsin or trypsin and device processing. Cells were seeded at 10,000 cells/well in 96 well plates and initial images were captured 2 hours after seeding at 10x magnification. Additional images were taken once per day over the following 3 days during growth.

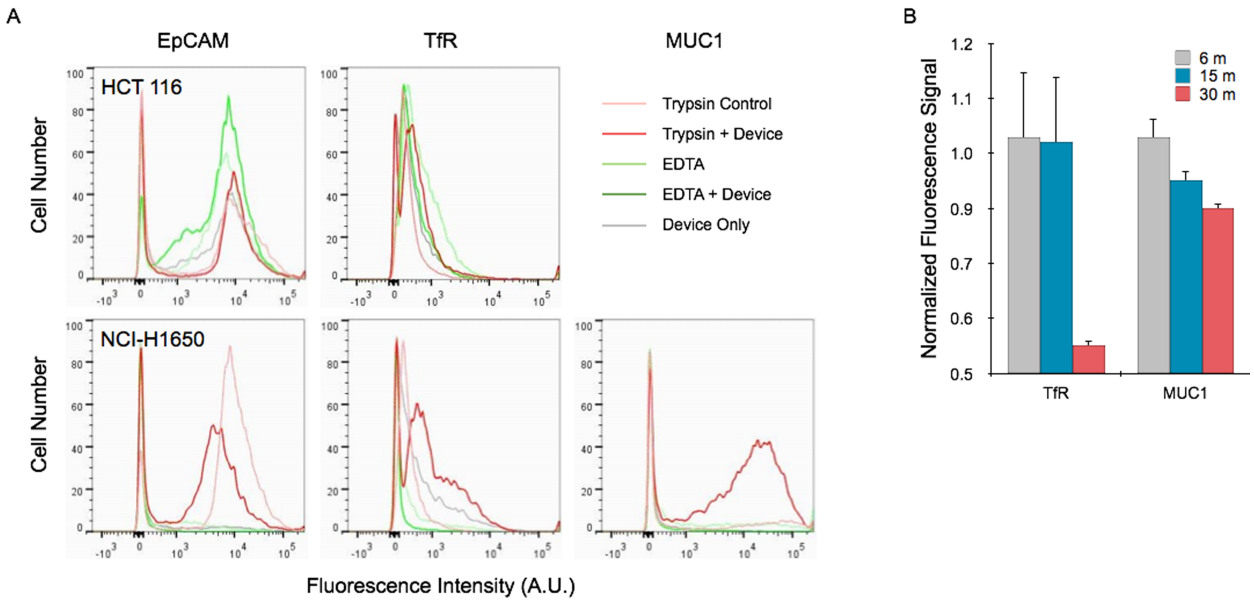

Figure S8. Biomarker analysis using flow cytometry. (A) Representative flow cytometry histograms for detection of EpCAM, TfR, and MUC1 on HCT 116 and NCI-H1650 cells obtained from spheroids under the indicated dissociation conditions. Normalized fluorescence signals, averaged from several experiments, are shown in Figure 6D and E. (B) NCI-H1650 spheroids were stained for TfR and MUC1 following prolonged digestion with trypsin, demonstrating that longer treatments lead to more pronounced decreases in expression for these trypsin-sensitive surface proteins. Error represent the standard error from at least three independent experiments.